Improved di-neutron cluster model for ^{6}He scattering

A. M. Moro,[1] K. Rusek,[2] J. M. Arias,[1] J. Gómez-Camacho,[1] and M. Rodríguez-Gallardo[3]

[1]*Departamento de Física Atómica, Molecular y Nuclear, Facultad de Física, Universidad de Sevilla, Apartado 1065, E-41080 Sevilla, Spain*
[2]*Department of Nuclear Reactions, Andrzej Soltan Institute for Nuclear Studies, Hoza 69, PL-00681 Warsaw, Poland*
[3]*Centro de Física Nuclear da Universidade de Lisboa, Lisbon P-1649-003, Portugal*

The structure of the three-body Borromean nucleus ^{6}He is approximated by a two-body di-neutron cluster model. The binding energy of the $2n$-α system is determined to obtain a correct description of the $2n$-α coordinate, as given by a realistic three-body model calculation. The model is applied to describe the breakup effects in elastic scattering of ^{6}He on several targets, for which experimental data exist. We show that an adequate description of the di-neutron-core degree of freedom permits a fairly accurate description of the elastic scattering of ^{6}He on different targets.

I. INTRODUCTION

The scattering of a weakly bound projectile by a target represents a challenging as well as an interesting problem in nuclear physics. A proper understanding of the process requires an accurate description of the structure of the projectile, including all bound and unbound states that can be effectively coupled during the collision. In the case of weakly bound two-body projectiles the problem has been solved using the Continuum Discretized Coupled-Channels (CDCC) method [1–3]. Within the CDCC method, the reaction process of a loosely bound two-body projectile by a structureless target is treated within a three-body picture. The idea of the method is to represent the continuum part of the two-body projectile spectrum by a finite set of square integrable states. These states are then used to generate the diagonal as well as the nondiagonal coupling potentials that enter the system of coupled equations.

In principle, the method can be extended to three-body projectiles. This will be the case, for instance, of Borromean nuclei, consisting of loosely bound and spatially extended three-body systems, typically composed of a compact core plus two weakly bound neutrons ($n + n + c$), and with no bound binary subsystems. In this case, a description of the three-body spectrum of the projectile is required. However, the calculation of the unbound spectrum of a three-body system is a very complicated problem by itself. In general, each physical state will be a complicated superposition of many channels with all possible spin and orbital angular momenta configurations. The calculation of the coupling potentials and the solution of the set of coupled equations in this large basis represents a complicated task. Despite these difficulties, in two recent works [4,5], this method has been applied to describe the scattering of ^{6}He on ^{12}C and ^{209}Bi. These calculations reproduce successfully the existing elastic scattering data for these reactions and represent an important advance toward the understanding of few-body nuclear reactions.

Most of the complexity of these processes involving Borromean nuclei arises from the fact that these systems exhibit many excitation modes, which can be associated with two different degrees of freedom: the n-n relative motion, and

the (nn)-c motion. In general, both modes will be excited during the collision. However, when the system is scattered by a medium mass or heavy target, the projectile-target interaction will excite mainly the coordinate between the neutrons and the core, because the repulsive Coulomb interaction will tend to repel the charged core, while the neutrons can approach closer to the target. Moreover, the nuclear interaction will attract more strongly the weakly bound neutrons. So, the net effect of the interaction with the target will be to stretch the nn-c coordinate, pushing the core apart from the target and pulling the neutrons close to it. Thus, a description of the projectile excitation mechanism that takes into account explicitly the nn-c coordinate should explain the main features of the reaction mechanism of the three-body system with the target.

Given the complexity of the full CDCC calculations with three-body projectiles, the development of these simple models can be very helpful to understand the main features of these processes by retaining only the essential ingredients to keep the model realistic.

In this work we revisit the so called di-neutron model for the ^{6}He case. In Sec. II, we address the problem of the ^{6}He structure within a three-body model. In Sec. III, we review the di-neutron model for this nucleus, and we propose a method to improve the accuracy of the model, while keeping its simplicity. In Sec. IV the new method is tested against existing experimental data for ^{6}He scattering on several targets. Finally, Sec. V is for summary and conclusions.

II. THREE-BODY MODEL FOR ^{6}He

Within a three-body picture, the wave function of the ^{6}He system can be conveniently expressed in terms of one of the Jacobi sets of coordinates. For the purposes of the present work, the most suitable representation is that in terms of the neutron-neutron relative coordinate, x, and the nn-^{4}He coordinate, y. This wave function, here denoted $\Psi^{3B}(x, y)$, can be obtained by solving the Schrödinger equation, using any of the methods proposed in the literature. Here, we followed the procedure proposed in Refs. [6] and [7], in which the wave

function is expanded in hyperspherical coordinates. The basic ingredient of the calculation are the two-body interactions between the subsystems (n-n and n-α). Besides the two-body potentials, the model Hamiltonian also includes a simple central three-body force depending on the hyperradius. This is introduced to overcome the underbinding caused by the other closed channels, such as the $t + t$ channel. The n-^{4}He potential is taken from Refs. [8] and [9], with central and spin-orbit components, and the neutron-neutron potential, with central, spin-orbit, and tensor components, from the prescription of Gogny, Pires, and Tourreil [10]. These calculations were performed with the code STURMXX [11], which uses the formalism described in Ref. [9]. The maximum hyperangular momentum was set to $K_{\max} = 20$ and the three-body force was adjusted to give the right binding energy. The calculated three-body wave function has a binding energy of $\epsilon_b = -0.955$ MeV and a rms point nucleon matter radius of 2.557 fm when assuming an α-particle rms matter radius of 1.47 fm. Further details of these calculations can be found in Refs. [9] and [12]. It should be noted that the three-body wave function is a complicated superposition of many channel configurations. Each channel is characterized by the angular momentum in the n-n and (nn)-α coordinates (l_x and l_y), the total orbital angular momentum (L), and the total spin of the neutron pair (S_x). In the ^{6}He ground state the dominant configuration corresponds to $S_x = l_x = l_y = 0$, which contributes to 80% of the norm.

To compare with the di-neutron model, presented below, we consider now the behavior of the wave function in the y coordinate. For this purpose, we calculate the probability density in the (nn)-α relative coordinate, y, here denoted as $\rho(y)$. This was calculated by integrating the square of the three-body wave function on the neutron-neutron coordinate, i.e.,

$$\rho^{3B}(y) = y^2 \int |\Psi^{3B}(x, y)|^2 dx \, d\Omega_y, \tag{1}$$

where $\Psi(x, y)$ is the total three-body wave function and Ω_y denotes the angular variables (θ_y, ϕ_y). This density is plotted in Fig. 1, depicted by the thick solid line. To illustrate the dominance of the $S_x = l_x = l_y = 0$ component, we show also the same quantity, retaining only this component in the wave function (thick dashed line). It can be noticed that, for $y > 5$ fm, the di-neutron density is completely determined by this component. Consequently, a realistic model for the ^{6}He ground state wave function must account, at least, for this configuration.

In scattering calculations involving the ^{6}He nucleus it is essential to include also a realistic description of the continuum states, given the large breakup probability of weakly bound nuclei. In the case of the Coulomb interaction, the response of the continuum to excitations of multipolarity λ is conveniently treated in terms of the reduced transition probability, $B(E\lambda)$ [13]. In Fig. 2 we consider the $B(E1)$ (upper panel) and $B(E2)$ (bottom panel) distributions, plotted as a function of the excitation energy of the ^{6}He nucleus with respect to the ground state. In both panels the full three-body calculation is depicted by the thick solid line. In these calculations, the continuum states were represented by true scattering wave functions, as
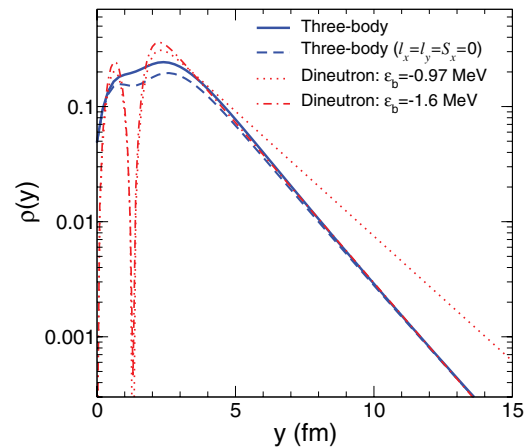

FIG. 1. (Color online) Neutron density in the di-neutron model, compared with a realistic three-body model. The di-neutron calculations use a Woods-Saxon potential with radius $R = 1.9$ fm and diffuseness $a = 0.25$ fm.

reported in Ref. [9]. The narrow peak in the $B(E2)$ corresponds to the known 2^+ low lying resonance.
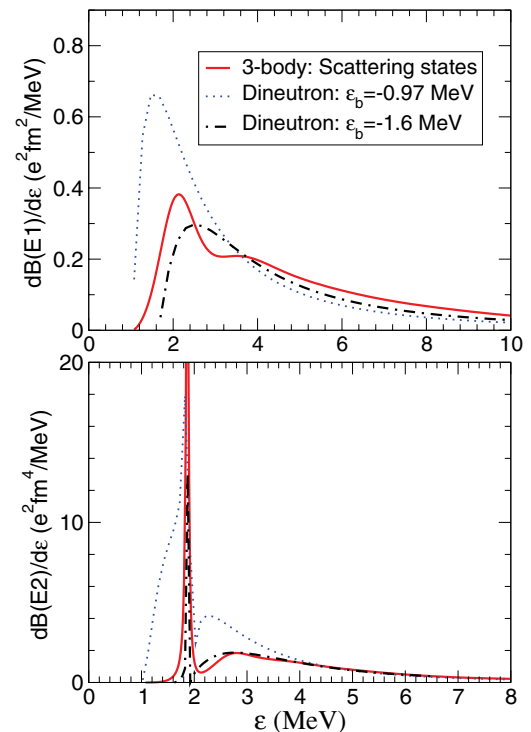

FIG. 2. (Color online) $B(E1)$ and $B(E2)$ transition strengths for the ^{6}He nucleus using different structure models. The solid lines correspond to the three-body calculation obtained with the *true* scattering states [9]. Di-neutron calculations using for the $2n$-α binding energy either the two-neutron separation energy (dotted-line) or the modified value $\epsilon_b = -1.6$ MeV (dotted-dashed line) are also shown.

III. THE DI-NEUTRON CLUSTER MODEL OF ^{6}He

We want to consider situations in which the (nn)-c degree of freedom is more relevant than the nn degree of freedom in ^{6}He. This is the case, for example, when electric operators are considered in structure calculations, or when Coulomb forces dominate in a collision. One could think then of approximating the three-body wave function by a product of two-body wave functions, i.e.,

$$\Psi^{3B}(x, y) \simeq \Psi^{2B}(y)\psi(x). \qquad (2)$$

The *di-neutron* model takes into account only the (nn)-c degree of freedom, whereas the relative motion between the two valence neutrons is ignored. This amounts to considering that the neutron pair remains in a highly correlated state $\psi(x)$ during the collision and, hence, excitations in this coordinate are not permitted. Moreover, the neutrons are assumed to be coupled to spin zero and bound to an inert α core in an s-wave relative motion, which, as we have seen before, is the dominant configuration in the ^{6}He ground state wave function. This model is inspired by the deuteron-α cluster model, which has been very successful in the description of ^{6}Li scattering within the continuum discretized coupled-channels method (e.g., Refs. [14–16]).

The problem in the di-neutron model lies in evaluating the wave functions, for the bound and continuum states, describing the motion of the halo neutrons relative to the α core, $\Psi^{2B}(y)$. Following the cluster model, one assumes that these wave functions can be obtained as the eigenstates of the Hamiltonian corresponding to a certain $2n$-α interaction. Typically, one assumes some reasonable geometry for the $2n$-α interaction and then adjusts the potential depth to obtain a given binding energy for the $2n$-α system.

In all the calculations presented here, the $\alpha + 2n$ interaction was parameterized using a standard Woods-Saxon form, with radius $R_0 = 1.90$ fm and diffuseness $a = 0.25$ fm, which corresponds to the set III of Ref. [17]. The ground state wave function was assumed to be a pure 2S configuration, because, due to the Pauli principle, the 1S state is forbidden.

So, the key question is: which is the binding energy that one should use for the $2n$-α system so that the corresponding wave function gives a reasonable description of ^{6}He in a di-neutron model?

In the application of the deuteron-α cluster model to ^{6}Li [14–16], one evaluates the binding energy for $d - \alpha$ just as the separation energy of ^{6}Li into $d + \alpha$. This is a reasonable procedure, which can be applied because the deuteron is bound by 2.2 MeV, which is more than the separation energy of ^{6}Li into $d + \alpha$, and so one can argue that the relative wave function of the valence proton and neutron within ^{6}Li is not very different from that in a free deuteron. Besides, the deuteron-α cluster model gives reasonable values for the mean square radii of ^{6}Li.

In the applications of the di-neutron model done so far to ^{6}He [17–22], the binding energy of the di-neutron has been taken as the two-neutron separation energy of ^{6}He, i.e., $|\epsilon_b| = S_{2n} = 0.975$ MeV. It should be noticed that, with this choice, one is assuming implicitly that the relative wave function of two neutrons within ^{6}He would be in a state similar to that of two neutrons with zero relative energy. This leads to an unrealistic wave function for the di-neutron-α motion, as discussed below.

The use of a binding energy $\epsilon_b = -0.975$ MeV yields the potential depth $V_0 = 93.51$ MeV. For the $\ell = 0$ and $\ell = 1$ continuum states we used the same potential as for the ground state. For the $\ell = 2$ continuum, the potential depth was changed to $V_0 = 91.25$ MeV, to get the 2^+ resonance at the value obtained in the the three-body calculation, which, in turn, is close to the experimental value ($\epsilon_x = 0.825$ MeV above the breakup threshold).

To illustrate this, we compare the density probability associated with the nn-c coordinate in the two- and three-body models. In the di-neutron model, the neutron density analogous to Eq. (1) is simply obtained as $\rho^{2B}(y) = |yR(y)|^2$, where $R(y)$ is the radial part of the wave function Ψ^{2B}. In Fig. 1, the density probability obtained with this model is given by the dotted line. When compared to the realistic three-body calculation (thick solid line) it becomes apparent that the former extends to considerably larger distances. For example, the rms associated with the di-neutron-α coordinate is 4.36 fm, considerably larger than the prediction of the three-body model, 3.25 fm. In view of this result, it is not surprising that the coupling of the ground state wave function with the dipole continuum states is unphysically enhanced in the two-body model.

This is indeed the case, as we can see in Fig. 2. In both panels, the dotted line corresponds to the di-neutron model. These distributions clearly overestimate both the $E1$ and $E2$ strengths predicted by the three-body model (thick solid lines). Not surprisingly, previous attempts to describe ^{6}He scattering by heavy targets [23,24] using this model showed that this simplified description of the ^{6}He nucleus tends to overestimate the effect of the continuum couplings. In Ref. [22] it was shown that by reducing the strength of the dipole couplings the agreement with the data could be significantly improved.

We consider that the $2n$-α binding energy used in the di-neutron model should not be given by the two-neutron separation energy. The di-neutron system that appears in ^{6}He is a correlated state, which, in the absence of the α particle, will be given by a wave packet with positive expectation value of the energy. Thus, the actual $2n$-α binding energy should be more negative, to compensate for the positive energy of the di-neutron. We propose to obtain $2n$-α binding energy to reproduce the known properties of the ^{6}He system, such as the rms radius and the transition strengths, within the di-neutron model. Asymptotically, the di-neutron wave function behaves as $\propto \exp(-ky)$, with $k = \sqrt{2\mu|\epsilon_b|}/\hbar$ and μ the $2n$-α reduced mass. Then, a natural choice for $|\epsilon_b|$ is to make the slope as close as possible to the three-body case. This leads to the value $|\epsilon_b| = 1.6$ MeV. The density calculated with this value, shown by the dotted-dashed line in Fig. 1, reproduces very well the three-body calculation (thick solid line) for separations beyond 4 fm. The di-neutron-α mean square separation obtained with the new wave function is reduced to 3.4 fm, in much better agreement with the three-body result. With the new binding energy, the depth of the s wave is modified to $V_0 = 96.06$ MeV. Again, this depth was used for the p waves. The depth of the $\ell = 2$ potential had to be changed to $V_0 = 92.7$ MeV to get

the 2^+ resonance at the correct excitation energy with respect to the ground state.

We note that, among the three geometries proposed in Ref. [17], namely, set I ($a = 0.65$ fm), set II ($a = 0.39$ fm), and set III ($a = 0.25$ fm), the latter is found to reproduce more accurately the three-body density. The other two geometries, having a larger diffuseness, give rise to a higher rms, even after modification of the two-neutron separation energy to correct the slope of the di-neutron density.

It can be seen that, with this geometry and binding energy, the $E1$ and $E2$ transition strengths are also well reproduced. This is shown in Fig. 2 by the dotted-dashed lines. It is observed that this increase of the binding energy reduces both strengths, showing a much better agreement with the prediction of the three-body calculation. Note that, because of the modification of the binding energy, the breakup threshold appears at a higher energy in our di-neutron model. So, the di-neutron model does not describe the low-energy continuum of ^{6}He, which is below 1.6 MeV excitation energy. However, it describes fairly well the continuum around the maximum of the $B(E1)$ distribution (2 MeV) and beyond.

IV. CALCULATIONS

In the remaining, we compare the two-body models discussed above with the elastic scattering data for several reactions induced by ^{6}He. In all the calculations presented here, we used the geometry of the $2n$-α potential with the smaller diffuseness ($a = 0.25$ fm). All these calculations are performed within the standard CDCC method [1].

We first consider the reaction ^{6}He + ^{64}Zn at Coulomb barrier energies, which was recently measured by Di Pietro *et al.* [25]. The ^{6}He ($=2n + \alpha$) continuum was discretized into $N = 7$ energy bins, evenly spaced in the asymptotic momentum k, and up to a maximum excitation energy of $\epsilon_{max} = 7$ MeV. We included s, p, and d waves for the $2n$-α relative orbital angular momentum. Inclusion of f waves had a negligible effect on the elastic angular distributions.

In these calculations, the $\alpha + {}^{64}$Zn interaction was taken from the optical model fit performed in Ref. [25]. For the $2n + {}^{64}$Zn interaction, we used the parameters of the $d + {}^{56}$Fe potential obtained in Ref. [26]. Diagonal as well as nondiagonal potentials were derived from these potentials by means of a single-folding method, as described elsewhere [17]. The coupled equations were integrated up to 100 fm and used 50 partial waves for the projectile-target relative motion. These calculations were performed with the code FRESCO [27].

In Fig. 3 we show the results for the elastic scattering angular distribution at the laboratory energies $E = 10$ and 13.6 MeV, along with the data of Di Pietro *et al.* [25]. For each energy three curves are shown: the dashed line is the cluster-folded calculation in which the projectile-target interaction is folded with the ground-state density of the ^{6}He nucleus, without inclusion of the continuum. At the higher energy this calculation exhibits a pronounced rainbow that is not observed in the data. Moreover, at both energies these calculations clearly underestimate the data at backward angles. Inclusion of the continuum within the conventional di-neutron model
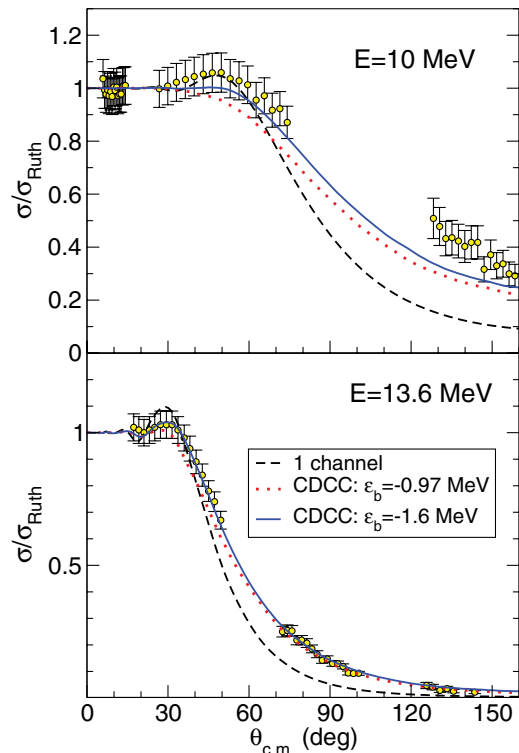

FIG. 3. (Color online) Elastic scattering angular distribution, divided by the Rutherford cross section, for the reaction ^{6}He + ^{64}Zn at $E = 10$ and 13.6 MeV. The dashed line is the cluster-folding calculation without inclusion of the continuum. The dashed line and the thick solid line are the di-neutron model calculations using the binding energy $\epsilon_b = S_{2n} = -0.975$ MeV and the modified binding energy $\epsilon_b = -1.6$ MeV, respectively. The experimental data are taken from Ref. [25].

(dotted lines) improves the agreement at backward angles, but reduces too much the cross section at the rainbow, thus underpredicting the data. This effect is a direct consequence of the overprediction of the $B(E1)$ distribution in the di-neutron model, as explained above. Finally, the thick solid line is the CDCC calculation with the di-neutron model with a modified binding energy ($\epsilon_b = -1.6$ MeV). This calculation improves the agreement at the rainbow, particularly at $E = 13.6$ MeV. At $E = 10$ MeV, this calculation slightly underestimates the data at backward angles, but we could not find an explanation for this discrepancy.

Next, we study the ^{6}He + ^{208}Pb, ^{209}Bi, and ^{197}Au reactions, which were recently analyzed in Ref. [22]. In Fig. 4 we present the calculations for the Pb and Bi targets, along with the experimental data from Kakuee *et al.* [28] and Aguilera *et al.* [29], respectively. Details of the fragment-target optical potentials and binning scheme can be found in Ref. [22]. The meaning of the lines is the same as in Fig. 3. In both cases, the calculation without continuum displays a marked rainbow that is not observed in the data. We have added also a calculation without continuum, but with the modified binding energy $\epsilon_b = -1.6$ MeV (thin solid line). This calculation illustrates the *static* effect caused by the change in the ground state wave function produced by the modification of the binding
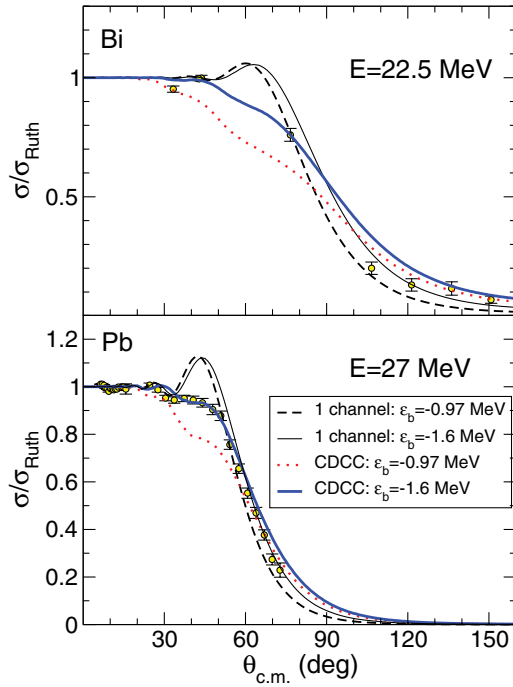
FIG. 4. (Color online) Elastic scattering angular distribution, divided by Rutherford cross section, for the reactions ^{6}He + ^{209}Bi at $E = 22.5$ MeV (top) and ^{6}He + ^{208}Pb at $E = 27$ MeV (bottom). The dashed line is the calculation without inclusion of the continuum, using the binding energy $\epsilon_b = -0.97$ MeV. The thin solid line is a similar calculation, but with $\epsilon_b = -1.6$ MeV. The dotted line and the thick solid line are the di-neutron model calculations using the binding energy $\epsilon_b = S_{2n} = -0.975$ MeV and the modified binding energy $\epsilon_b = -1.6$ MeV, respectively. Experimental data are from Refs. [28] and [29].

FIG. 5. (Color online) Elastic scattering angular distribution, divided by the Rutherford cross section, for the reaction ^{6}He + ^{197}Au at $E = 27, 29,$ and 40 MeV. The dashed line is the cluster-folding calculation without inclusion of the continuum. The dotted line and the thick solid line are the calculations using the di-neutron model with $\epsilon_b = -S_{2n} = -0.975$ MeV and $\epsilon_b = -1.6$ MeV, respectively. The experimental data are taken from Ref. [30].

energy. Qualitatively, these two calculations are very similar. In particular, the pronounced rainbow is still present in the new calculation. The similitude between these two calculations indicates that the trend of the data can not be simply explained by changing the size of the di-neutron-α wave function and, consequently, dynamical effects are indeed very important. Inclusion of the continuum within the conventional di-neutron model (dotted line) produces a strong reduction of the cross section at intermediate angles, largely underestimating the data. As noted above, this is caused by the overestimation of the dipole couplings in this model. In the modified di-neutron model the rainbow is also suppressed, but the final result is in very good agreement with the data.

Finally, we discuss the results for the ^{6}He + ^{197}Au reaction at $E = 27, 29,$ and 40 MeV and compare them with the data of Ref. [30]. The lines have the same meaning as in Figs. 3 and 4. Similarly to the case of the lead target, at $E = 27, 29$ MeV, the one channel calculation exhibits a pronounced rainbow, which is almost absent in the data. This effect is very well accounted for in the modified di-neutron calculation. At $E = 40$ MeV, the rainbow is suppressed somewhat, but not completely, in the full CDCC calculation. The lack of data at the relevant angles does not permit us to make strong conclusions about the existence of the rainbow, but the agreement between the
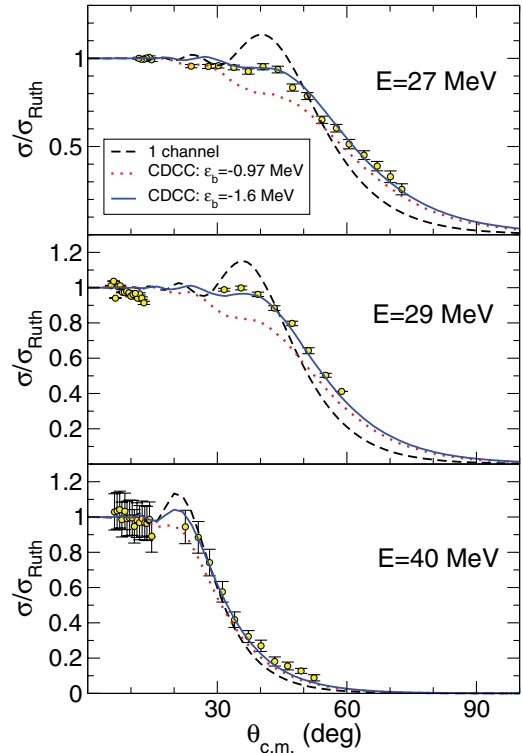
data and the calculation is fairly good where the comparison is possible.

It is interesting to note that the underestimation of the data in the conventional di-neutron model is more pronounced at lower energies. This is because at lower energies dipole Coulomb couplings become more important and, as we showed before, these couplings are unphysically enhanced in the conventional di-neutron model.

All these calculations show that the proposed model describes fairly well the elastic data for different targets and could even be used as a predictive tool for reactions for which data do not exist. The good agreement with the data clearly supports the idea, anticipated in the Introduction, that the degree of freedom that enters actively in the elastic scattering of Borromean systems on medium mass and heavy targets is that for the relative motion between the halo neutrons and the core.

V. SUMMARY AND CONCLUSIONS

In this work, we have studied the application of the di-neutron model to describe ^{6}He structure and scattering. We find that, when the di-neutron model is applied assuming for the $2n$-α binding energy the two-neutron separation energy of ^{6}He, the description of the structure of ^{6}He obtained is

not in agreement with the results of a realistic three-body calculation. One obtains an unrealistically long tail of the $2n$-α relative wave function and too large values of the $B(E1)$ and $B(E2)$ distributions. When this model of ^{6}He is used in scattering calculations, the couplings between the ground state and the continuum states are overestimated, and this produces too much absorption from the elastic channel.

We have proposed a modified di-neutron model in which the $2n$-α binding energy is set to reproduce the density distribution in the $2n$-α coordinate given in a realistic three-body model. We find that a $2n$-α binding energy of 1.6 MeV produces a rms and $B(E1)$ and $B(E2)$ distributions that are similar to those obtained in a realistic three-body calculation.

The model has been tested for several reactions induced by ^{6}He, providing in all cases a very good description of the elastic scattering data. These results indicate that, despite its simplicity, the model can provide a useful and reliable description of reactions involving the ^{6}He nucleus. Using an identical procedure, the method could be also extended to other Borromean systems, such as ^{11}Li or ^{14}Be.

We would like to emphasize that the present model is not intended to replace the realistic three-body calculations for the scattering of Borromean nuclei. The development of these models, although numerically more demanding, are of great importance for a full quantitative understanding of these processes. However, we believe that simple models, such as those discussed here, are also very useful to provide us with a transparent physical interpretation of these collisions.

[1] M. Yahiro, Y. Iseri, H. Kameyama, M. Kamimura, and M. Kawai, Prog. Theor. Phys. Suppl. **89**, 32 (1986).

[2] M. Kamimura, M. Yahiro, Y. Iseri, Y. Sakuragi, H. Kameyama, and M. Kawai, Prog. Theor. Phys. Suppl. **89**, 1 (1986).

[3] N. Austern, Y. Iseri, M. Kamimura, M. Kawai, G. Rawitscher, and M. Yahiro, Phys. Rep. **154**, 125 (1987).

[4] T. Matsumoto, E. Hiyama, K. Ogata, Y. Iseri, M. Kamimura, S. Chiba, and M. Yahiro, Phys. Rev. C **70**, 061601(R) (2004).

[5] T. Matsumoto, T. Egami, K. Ogata, Y. Iseri, M. Kamimura, and M. Yahiro, Phys. Rev. C **73**, 051602(R) (2006).

[6] M. V. Zhukov, B. V. Danilin, D. V. Fedorov, J. M. Bang, I. J. Thompson, and J. S. Vaagen, Phys. Rep. **231**, 151 (1993).

[7] I. J. Thompson, F. M. Nunes, and B. V. Danilin, Comput. Phys. Commun. **161**, 87 (2004).

[8] J. Bang and C. Gignoux, Nucl. Phys. **A313**, 119 (1979).

[9] I. J. Thompson, B. V. Danilin, V. D. Efros, J. S. Vaagen, J. M. Bang, and M. V. Zhukov, Phys. Rev. C **61**, 024318 (2000).

[10] D. Gogny, P. Pires, and R. de Tourreil, Phys. Lett. **B32**, 591 (1970).

[11] I. J. Thompson, STURMXX code, 2004. Available at http://www.fresco.org.uk.

[12] M. Rodríguez-Gallardo, J. M. Arias, J. Gómez-Camacho, A. M. Moro, I. J. Thompson, and J. A. Tostevin, Phys. Rev. C **72**, 024007 (2005).

[13] D. M. Brink and G. R. Satchler, *Angular Momentum* (Oxford University Press, USA, 1994).

[14] Y. Sakuragi, M. Yahiro, and M. Kamimura, Prog. Theor. Phys. (Kyoto) **68**, 322 (1982).

[15] Y. Sakuragi, Phys. Rev. C **35**, 2161 (1987).

[16] N. Keeley and K. Rusek, Phys. Lett. **B375**, 9 (1996).

[17] K. Rusek, K. W. Kemper, and R. Wolski, Phys. Rev. C **64**, 044602 (2001).

[18] R. S. Mackintosh and K. Rusek, Phys. Rev. C **67**, 034607 (2003).

[19] K. Rusek, N. Alamanos, N. Keeley, V. Lapoux, and A. Pakou, Phys. Rev. C **70**, 014603 (2004).

[20] R. S. Mackintosh and N. Keeley, Phys. Rev. C **70**, 024604 (2004).

[21] L. Giot *et al.*, Phys. Rev. C **71**, 064311 (2005).

[22] K. Rusek, I. Martel, J. Gómez-Camacho, A. M. Moro, and R. Raabe, Phys. Rev. C **72**, 037603 (2005).

[23] K. Rusek, N. Keeley, K. W. Kemper, and R. Raabe, Phys. Rev. C **67**, 041604(R) (2003).

[24] N. Keeley, J. M. Cook, K. W. Kemper, B. T. Roeder, W. D. Weintraub, F. Marechal, and K. Rusek, Phys. Rev. C **68**, 054601 (2003).

[25] A. Di Pietro *et al.*, Phys. Rev. C **69**, 044613 (2004).

[26] S. I. Al-Quraishi, C. E. Brient, S. M. Grimes, T. N. Massey, J. Oldendick, and R. Wheeler, Phys. Rev. C **62**, 044616 (2000).

[27] I. J. Thompson, Comput. Phys. Rep. **7**, 167 (1988).

[28] O. R. Kakuee *et al.*, Nucl. Phys. **A728**, 339 (2003).

[29] E. F. Aguilera *et al.*, Phys. Rev. Lett. **84**, 5058 (2000).

[30] R. Raabe, Ph.D. thesis, Katholieke Universiteit Leuven, 2001.